Reports

BioTechniques

Improved SARS-CoV-2 PCR detection and genotyping with double-bubble primers

Menachem Ailenberg[1], Andras Kapus[1] & Ori D Rotstein*,[1]

*[1]Keenan Research Centre for Biomedical Science of St Michael's Hospital, Unity Health Toronto & The Departments of Surgery, St Michael's Hospital & The University of Toronto, Toronto, Canada; *Author for correspondence: Tel.: +1 416 864 5637; ori.rotstein@unityhealth.to*

BioTechniques 71: 00–00 (November 2021) 10.2144/btn-2021-0063

First draft submitted: 6 July 2021; Accepted for publication: 1 August 2021; Published online: 13 September 2021

ABSTRACT

A new approach for improved RT-PCR is described. It is based on primers designed to form controlled stem–loop and homodimer configurations, hence the name 'double-bubble' primers. The primers contain three main regions for efficient RT-PCR: a 3′ short overhang to allow reverse transcription, a stem region for hot start and a template-specific region for PCR amplification. As proof of principle, *GAPDH*, SARS-CoV-2 synthetic RNA and SARS-CoV-2 virus-positive nasopharyngeal swabs were used as templates. Additionally, these primers were used to positively confirm the N501Y mutation from nasopharyngeal swabs. Evidence is presented that the double-bubble primers offer fast, specific, robust and cost-effective improvement in RT-PCR amplification for detection of gene expression in general and for diagnostic detection and genotyping of SARS-CoV-2 in particular.

METHOD SUMMARY

A new approach for improved RT-PCR is described. It is based on primers designed to form controlled stem–loop and homodimer configurations hence the name 'double-bubble' primers. It is fast, specific, robust and cost-effective. The method is applied to detect wild-type and mutated SARS-CoV-2 virus.

KEYWORDS:

cost-effective PCR ● double-bubble PCR primers ● fast PCR ● hot-start PCR ● RT-qPCR ● SARS-CoV-2

RT-PCR-based techniques are used to detect gene expression in diagnostic as well as research labs. Ideally, they are highly accurate, avoiding false-negative and false-positive results, thereby affording early and accurate detection of gene expression. Conventional PCR primers are designed to avoid creation of homo- and hetero-primer dimers [1]. When primers dimerize with 5′ overhangs, the polymerase fills in the overhangs, thus changing the sequence of the 3′ end of the primers such that they can no longer serve their specific goal of extension by the polymerase. In order to obtain specificity of the PCR reaction, various hot-start approaches have been proposed [2]. A variety of techniques are based on the stem–loop DNA configuration including, for example, hot-start PCR with improved specificity [3], quantification of miRNAs [4] or real-time PCR detection probes [5]. The above publications assume the stem–loop configuration as a basis for their methods. We reasoned that a more stable configuration than the stem–loop primer is its homodimer configuration. This distinction is important since the homodimer is more thermodynamically stable (i.e., it has a higher melting temperature).

SARS-CoV-2 is a highly transmissible and pathogenic coronavirus that emerged in late 2019 and has caused a pandemic of acute respiratory disease, named COVID-19, which threatens human health and public safety [6]. Effective, sensitive and reliable diagnostic reagents are of paramount importance for combating the ongoing COVID-19 pandemic. Based on genotyping of 31,421 SARS-CoV-2 genome samples collected up to 23 July 2020, Wang *et al.* revealed that essentially all of the current COVID-19 diagnostic targets have undergone mutations [7].

In the current studies, our primers are designed, against conventional assumptions, to deliberately create mixed primers with intramolecular stem–loop bubble and intermolecular homodimer bubble configurations, both with 3′ overhangs that allow reverse-transcription and thus one-step RT-PCR. The segments of both monomer and dimer primer configurations form non-annealed bubbles. We refer to these primer configurations as double-bubble (D-B) primers. We performed exhaustive PCR experiments (different gene targets and regions, assorted primers, one- or two-step, end point or real-time, TaqMan® or SYBR® Green, standard or fast conditions, normal versus hot-start, cheap versus expensive Taq polymerases) to show the efficacy of the D-B primers in detecting and genotyping SARS-CoV-2 and to demonstrate that these primer configurations offer fast, specific, robust and cost-effective improvement in PCR amplification.

Materials & methods

Materials

All reagents were purchased from Millipore-Sigma (Oakville, ON, Canada) unless otherwise stated. Primers were purchased from Millipore-Sigma or Integrated DNA Technologies (CA, USA). VIC-TqM–NFQ-MGB probe, FAM-TqM–NFQ-MGB probe, SYBR Green 2× mix, ROX reference dye, dNTPs, DNase I and ultra-low-range DNA ladder were from Thermo Fisher Scientific (MA, USA). Taq polymerases were part of the PCR kits (SYBR Green standard [4367659], Fast [4472908]) and TaqMan kits: Gene Expression + uracil-DNA glycosylase (UDG) (4369016), Fast Advanced (A44360), Fast Advanced + UDG (4444557); all Thermo Fisher Scientific. Non-hot-start Taq polymerases were from FroggaBio (ON, Canada) and New England BioLabs (NEB; ON, Canada). The 100-bp DNA ladder was from FroggaBio. iScript reverse transcriptase was a product of Bio-Rad Laboratories (ON, Canada). SARS-CoV-2 synthetic RNA: ORF, E, N, 8.0×10^5 genome copies/μl was from ATCC (VR-3276SD; VA, USA).

Primers & TaqMan probes design

We designed D-B as well as conventional control PCR primers from two main regions of the SARS-CoV-2 genome, namely the N (nucleoprotein) gene and the S (spike) gene. A few primers were designed and utilized interchangeably in order to further demonstrate the efficacy of the D-B primers. Two TqM probes were also designed. The maximal length allowed for TqM probes is 45 nt, since the reporter dye on longer probes is considered too far from the nonfluorescent quencher (NFQ) molecule and thus it is not quenched. The VIC-TqM-NFQ-MGB probe #12 from region 1 has 45 nucleotides and the FAM-TqM–NFQ-MGB probe #13 from region 2 has 44 nucleotides. Primer analysis was performed using Oligo Analyzer Version 3.1 from Integrated DNA Technologies. For example, antisense primer 8′ was designed to form stem–loop and homodimer configurations with free energy ΔG = -6.34 and -10.01 kcal/mol, respectively. The annealing temperature to its target was 73.5°C. Its counterpart, sense primer 8, had similar values. It should be noted that the primer set 8 and 8′ form a few heterodimers; the most stable of them has ΔG = -7.81 kcal/mole. This is inconsequential to the PCR reaction as long as the heterodimer is less stable than the specific primers and the heterodimers do not form a stable 5′ overhang that would annul the primers. This is also not consequential to the primers' performance in the PCR reaction because the reaction is cycled between 95 and 70°C, temperatures at which the nonspecific heterodimer would melt. The primers' assignments and locations are elaborated in Supplementary Figure 2 & Supplementary Table 1.

RT-PCR protocols

RNA was extracted from Huh cells (ATCC) using RNeasy extraction kit (Qiagen, ON, Canada). Virus RNA was extracted from heat-inactivated nasopharyngeal swabs (kindly supplied by St. Michael's Hospital molecular diagnostic lab) using Monarch® RNA Cleanup Kit (NEB). TqM probe and primers were used at concentrations of 0.9 and 0.3 μM, respectively. RT-PCR including real-time qPCR was performed under standard or fast conditions in a 10-μl reaction. Standard conditions were: 95°C, 10 min, then 40 cycles of 95°C, 15 s and 70°C, 1 min. Fast conditions were: 95°C, 20 s, then 30 cycles of 95°C, 1 s and 70°C 20 s. For one-tube RT-PCR a 42°C, 15 min → 95°C, 1 min pre-cycling step was added. For end point RT-PCR, an additional stage of 72°C, 5 min → 4°C hold was added. PCR was performed with UDG to avoid DNA carryover adding a 50°C, 5 min → 95°C, 1 min pre-cycling step. One-tube RT-PCR was performed without UDG to avoid possible degradation of the nascent cDNA. For cDNA synthesis, iScript reverse-transcriptase kit was employed: 25°C, 5 min, 42°C, 15 min 95°C, 1 min, 4°C hold (BioRad, 1708891). RT-PCR individual protocol changes are elaborated in the 'Results & discussion' section as well as in the figure legends. Reverse transcription and end point PCR were performed with a Veriti 96-well thermal cycler, and real-time RT-qPCR was performed with Quant Studiob7 Flex (both Thermo Fisher Scientific).

Results & discussion

D-B primer design

We have shown previously that stem–loop (also known as panhandle, hairpin, loop-incorporated, bulge or bubble) primer configurations offer a more specific hot start for PCR reactions [3]. However, with this blunt-end configuration, it is not possible to use the primers for reverse transcription. We therefore wished to include a 3′ overhang to enable reverse transcription from this primer and thus provide the option of one-tube RT-PCR. It has been shown that self-complementary DNA octamers can occur in both hairpin and dimer configurations under suitable concentrations and temperatures [8]. However, techniques that employ stem–loop primers have usually overlooked the dimer configuration [3,4,9]. We surmised that in addition to the self-annealing stem–loop monomer, a more thermodynamically stable configuration of a primer dimer exists in our system (Figure 1A & Supplementary Figure 1A & B). Recognizing the existence of the more stable homodimer is crucial for primer design because its annealing temperature is higher than that of the stem–loop configuration. The primers in both configurations create D-B primers.

In order to show experimentally the existence of both primer configurations, we performed a melt curve experiment with consecutive double dilutions of D-B antisense primer #8 (Figure 1D & Supplementary Figure 2 & Supplementary Table 1). Melt curve is performed in the PCR machine, mixing the oligos with SYBR Green, a dye that binds preferentially to double-stranded DNA, resulting in emitted fluorescence that is proportional to the number of Watson–Crick base pairings. A similar technique has been used with PicoGreen dye (which has similar properties to SYBR) to elucidate hairpin probes opening [10]. As can be noted in the derivative plot of the melt curve, at higher concentrations (Figure 1D: 10 μM), the derivative peak (turquoise arrow) was narrower. As the concentrations of the primer

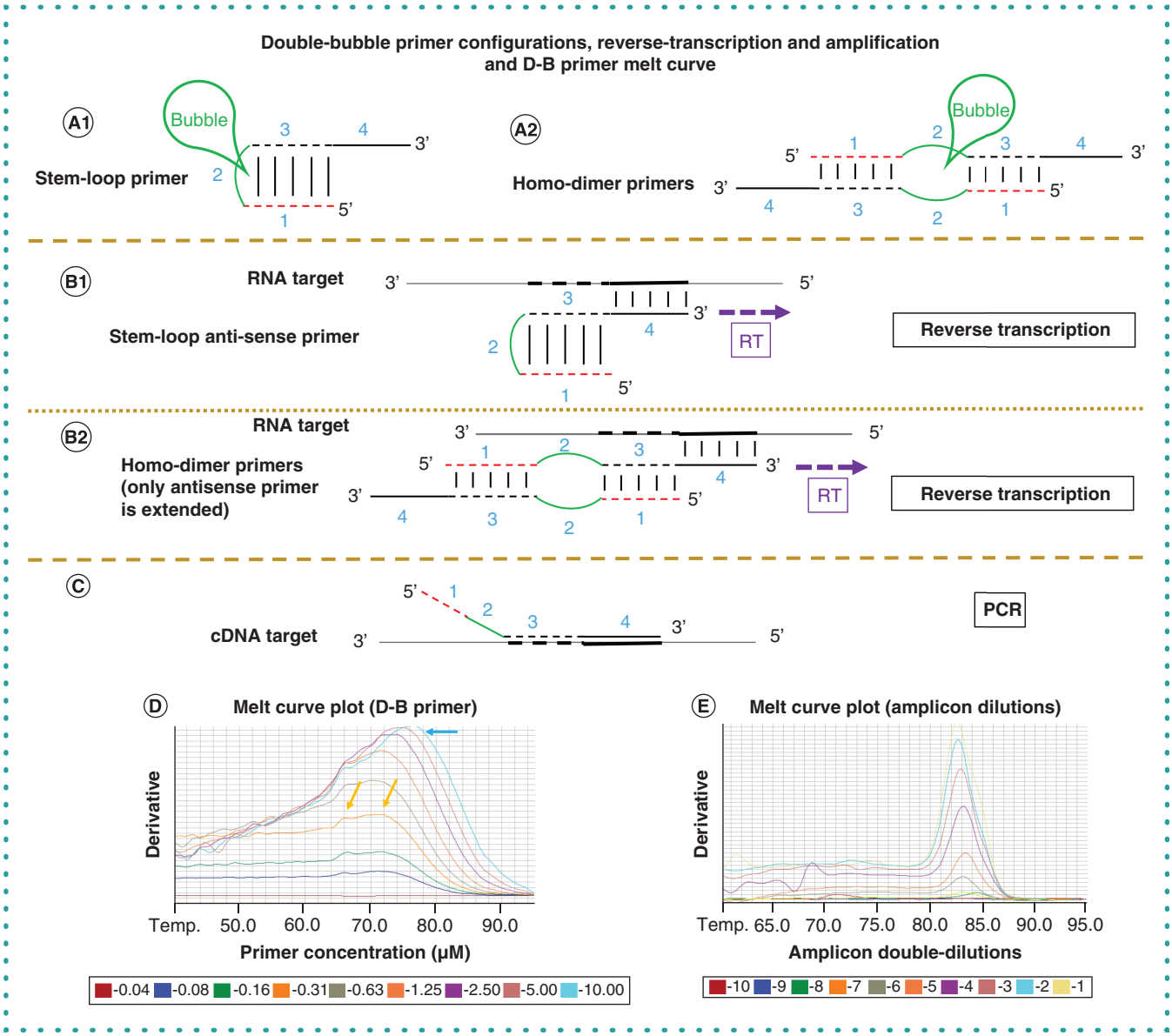

Figure 1. Double-bubble primer configurations, reverse transcription and amplification and melt curve of double dilutions of double-bubble anti-sense primer #8′ or PCR amplicon from SARS-CoV-2 synthetic RNA gene N. There are four regions to the D-B primer. Regions 3 and 4 are template-specific nucleotides. Region 4 is the 3′ overhang and region 3 is a self-annealing sequence to region 1. Region 2 is a random sequence that forms the non-annealed bubble in the self- and homo-dimer primer, hence 'double bubble' (D-B) primer. **(A)** Primer configurations: (1) stem–loop self-annealing; (2) homodimer head-to-tail annealing. **(B)** 3′ overhang of antisense primer annealed to RNA target during reverse transcription: (1) stem–loop primer; (2) homodimer primer. Note that in the homodimer configuration, each 3′ overhang can potentially anneal to the target RNA. **(C)** Primer annealed to cDNA target during PCR. Note that at the initial PCR cycles, only regions 3 and 4 are annealed to the template DNA, while in subsequent cycles, regions 1 through 4 are annealed to the PCR amplicon and amplified exponentially. **(D & E)** Melt curves: **(D)** antisense primer #8′ or **(E)** PCR amplicon were subjected to double dilutions. SYBR and ROX dyes were added and melt curve was performed. The data show derivative reporter. Note a left shift **(D)** of the derivative peak as a function of the concentration (0.04–10.00 μM) and temperature (40–95°C) indicating shifting of antisense primer #8′ from the homodimer to the stem–loop configuration. The Gibbs free energy for stem–loop and homodimer was ΔG = -6.34 and -10.01 kcal/mole, respectively. A melt curve was possible with the D-B primer because in both configurations it forms a double-stranded DNA that binds SYBR Green efficiently. In contrast, a single-stranded normal random-coiled DNA primer has lower binding affinity for SYBR green. Therefore, to compare versus a normal single amplicon as a control, we performed **(E)** a melt curve of double dilutions of a PCR amplicon (#1 the most concentrated, #9 the most diluted and #10 no amplicon), amplified from SARS-CoV-2 N synthetic RNA template using D-B primer mix #8. Note that there is no left shift in the peak as a function of concentration and temperature.

declined (e.g., at 0.31 μM) a broader peak was observed with two prominent peaks apparent (orange arrows in Figure 1D), consistent with more than one primer configuration. Moreover, with the declining temperatures, a temperature left shift of the peak was observed, consistent with a primer configuration shift to form more stem–loop configured primers (Supplementary Figure 1). This observation is consistent with previous publications suggesting that at high concentrations, there is a preference for the homodimer over the hairpin configuration [1,8,11]. It is interesting to note that the shift from the hairpin to the homodimer configuration was shown using polyethylene glycol, a reagent known to enhance the concentration of the oligo by molecular crowding [12]. In contrast, when a single PCR amplicon underwent double dilutions and was subjected to melt curve analysis (Figure 1E), no shifts in the derivative peaks were observed between the various concentrations and temperature changes, further confirming that the temperature left shifts of the derivative peaks of the D-B primer melt curve indicated the existence of at least two primer configurations. Similar results were obtained with double dilutions of amplicons derived from RT-PCR using SARS-CoV-2 RNA template and D-B primer mix #8 (Supplementary Figure 3).

Proof of principle of D-B primers with *GAPDH*

As preliminary proof of principle for the performance of the D-B primers in a PCR reaction, we designed *GAPDH* primers in both normal and D-B configurations (Supplementary Table 1: primer pairs 1 and 2, respectively). We utilized RNA from HuH-7 cells as template for the RT-PCR reaction. Of note, human *GAPDH* has 67 pseudogenes [13] and therefore genomic DNA can serve as template for a PCR reaction, with amplicons similar in size to cDNA that is reverse-transcribed from its mRNA. Supplementary Figure 4 compares end point PCR amplifications utilizing both normal and D-B primers on agarose gel. Both primers amplified the *GAPDH* template whether using a column-derived RNA preparation, known to contain contaminations of genomic DNA which in turn contains *GAPDH* pseudogenes (Supplementary Figure 4, lanes 2 and 3) or cDNA reverse-transcribed from DNase I-treated RNA (Supplementary Figure 4, lanes 6 and 7). When RNA preparation was treated with DNase I and subjected to PCR without reverse transcription, no *GAPDH* amplicon was detected, further showing the specificity of both normal and D-B primers. As expected, there was a size difference of the PCR amplicon between the normal and D-B primers (135 and 152 bp, respectively), and as a result of the amplicon size, the signal of the amplicon of the D-B primer was more intense than the normal primer, because it binds more SYBR Green molecules.

Validation of D-B primers using SARS-CoV-2 synthetic RNA N

In order to further assess the efficacy of the D-B primers, we performed an intra-assay reproducibility test using TaqMan qPCR in ten replicates with SARS-CoV-2 synthetic RNA as template and D-B primer mix #8. As can be observed in Supplementary Figure 5, high C_t reproducibility was achieved with the D-B primers (C_t mean $\pm$ SD = 31.950 $\pm$ 0.140; n = 10; coefficient of variation = 0.437%).

Next we utilized one-tube RT-qPCR using SARS-CoV-2 synthetic RNA as template with decimal dilutions of 8×10^5 to 8×10^2 copies per tube (Figure 2A–C) with D-B primer mix #8 from region 1 and VIC-TqM probe #12. The template was amplified in a dose-related manner, as shown in the amplification plot (Figure 2A). Figure 2B shows the PCR reaction products from Figure 2A in an agarose gel. Figure 2C depicts the plot of C_t values versus log RNA copy number. The slope of the equation -3.3359 represents 99.42% amplification efficiency with linearity of R^2 = 0.9816. We also used primer mix #10 and FAM-TqM probe #13 from region 2 to demonstrate one-tube RT-qPCR amplification of SARS-CoV-2 synthetic RNA N (Figure 2D). The amplification in the one-tube RT-qPCR reaction suggests that the reverse transcription reaction at 42°C (a temperature at which the primers are expected to be in D-B configurations) was primed by the 3′ overhang of the antisense D-B primers, as illustrated in Figure 1B.

Exploring D-B primers with fast PCR systems

One of the features that proved to be crucial during the COVID-19 pandemic was the need for prompt results of the PCR tests. In order to evaluate the D-B primers under rapid PCR conditions, we explored their performance with TqM fast systems. First, we used D-B primer mix #10 from region 2 with synthetic SARS-CoV-2 cDNA equivalent to 2×10^4 RNA copies as template with TqM probe #13 and TqM fast kit (Figure 3A). Amplification was noted both at the real-time amplification plot and agarose gel (Figure 3A, insert). We also utilized D-B primer mix #8 in one-tube RT-qPCR with 2×10^5 synthetic RNA SARS-CoV-2 copies as template, TqM fast kit without UDG and TqM probe #12 (Figure 3B). Shown are the amplification plot as well as the agarose gel (Figure 3B, insert). We also studied real-time duplex qPCR using cDNA from SARS-CoV-2 synthetic RNA N as template, TqM fast kit with UDG and D-B primer mixes #8 and #10. Figure 3C & D show amplification plot and agarose gel of PCR, respectively; arrows indicate duplex amplification. Thus different D-B primers are compatible with fast one- and two-tube PCR as well as duplex amplification.

Next we explored the use of the D-B primers for SARS-CoV-2 detection in nasopharyngeal swabs from patients. Supplementary Figure 6A depicts the amplification plot of three decimal dilutions of cDNA reverse transcribed from virus RNA extracted from nasopharyngeal swab of patient S1, using SYBR Green qPCR with primer mix #8, and the efficiency plot (insert) with a slope of -3.2942 (101.17% efficiency, R^2 = 0.9934). Supplementary Figure 6B shows the melt curve of the PCR reaction suggesting one pure amplicon for each of the three dilutions.

We tested the D-B primers with the fast TqM system, using cDNA obtained from three nasopharyngeal swabs of patients (S1, S2, S3) who tested positive for SARS-CoV-2. Supplementary Figure 7A shows the amplification plot of patients' cDNAs and control cDNA from reverse-transcribed SARS-CoV-2 synthetic RNA, with D-B primer mix #8. We also tested the TqM fast kit with one-tube RT-qPCR with RNA

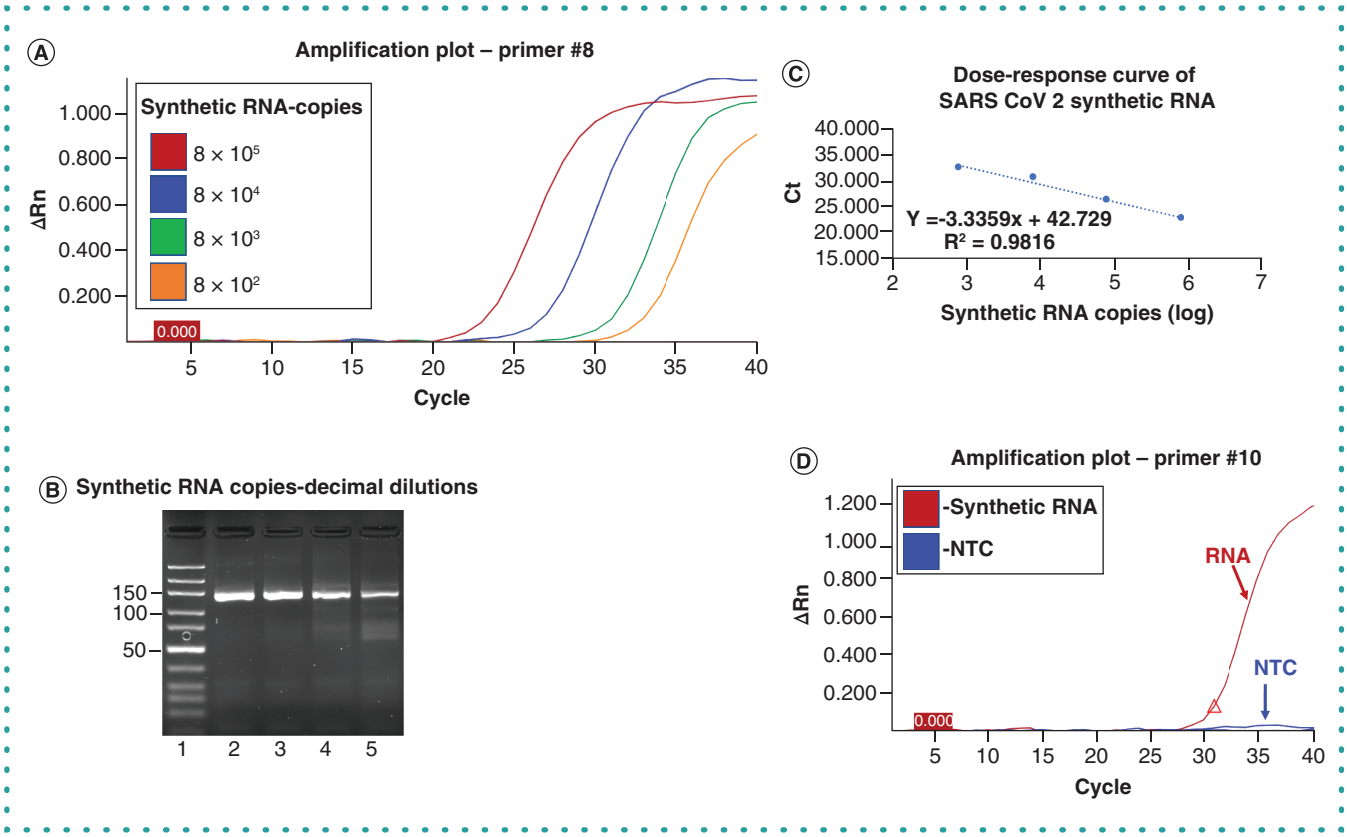

Figure 2. One-tube RT-qPCR using double-bubble primer mixes #8 and #10. (A–C) Dose–response curves using double-bubble primer mix #8 and VIC-TqM probe #12 and decimal dilutions of SARS-CoV-2 synthetic RNA N. **(A)** Real-time amplification plot. C_t values: 8×10^5 copies, 22.82; 8×10^4 copies, 26.27; 8×10^3 copies, 30.55; 8×10^2 copies, 32.51. **(B)** 5% agarose gel of the PCR amplification products. Lane 1: ultra-low-range ladder; lanes 2–5: 139-bp amplicons of 8×10^5 to 8×10^2 RNA copies per tube. Also included in the PCR reaction mix were 2× TqM buffer without UDP and iScript reverse-transcriptase. **(C)** Efficiency plot of the PCR reaction depicted in panel A. Slope = -3.3359 represents PCR reaction efficiency of 99.42%; $R^2 = 0.9816$. **(D)** One-tube RT-qPCR using double-bubble primer mix #10 from region 2 using SARS-CoV-2 synthetic RNA (2×10^4 copies per tube) and FAM-TqM probe #13. RT-qPCR was performed with standard conditions.

extracted from positive patient S2 and control synthetic RNA. Shown in Supplementary Figure 7B is the amplification plot as well as the agarose gels of the samples (insert).

We next evaluated the efficiency of the D-B primers in detecting SARS-CoV-2 with the fast TqM system. Figure 4 show a dose–response curve of decimal dilutions of SARS-CoV-2 RNA from the nasopharyngeal swab of patient S1. Synthetic RNA of the N gene of SARS-CoV-2 served as positive control. One-tube RT-qPCR using fast TqM buffer kit was performed. Figure 4A & B show the PCR amplification plot and agarose gel, respectively. Figure 4C shows the efficiency plot (slope = -3.1843, efficiency = 106.08%; $R^2 = 0.9988$). Compared with synthetic RNA and allowing for the sample dilutions, it is calculated that patient S1's nasopharyngeal swab contains 1.4×10^6 virus RNA copies per microliter, and the limit of detection is 3.76 SARS-CoV-2 virus copies per reaction.

To test the validity of several D-B primers from different regions of the SARS-CoV-2 genome to detect SARS-CoV-2 virus, we performed one-tube RT-qPCR with the TqM fast system (Figure 5). The primers are from both region 1 and 2 of the SARS-CoV-2 N gene (as specified in Supplementary Figure 2 & Supplementary Table 1). We used normal control primer mix #3, D-B primer mix #4 and D-B primer mix #8 from region 1; primer mixes #3, #4 and #8 can use the same VIC-TqM probe #12. We also used D-B primer mix #10 from region 2. Figure 5 shows the amplification plot as well the agarose gel with primer mixes #3, #4, #8 and #10 with SARS-CoV-2 RNA from patient S3. Note the amplifications with the D-B primer mixes #4, #8 and #10 and no amplification with the normal shorter primer mix #3 because of the high annealing/extension temperature used (70°C) as well as the shorter times for the cycling between 95 and 70°C, conditions that favor the longer D-B primers' performance. It should be noted that primer mix #3 contains the normal 20-nt primers that are routinely used in PCR reactions. The fact that they did not amplify under these conditions further demonstrates the advantage of using the D-B primers.

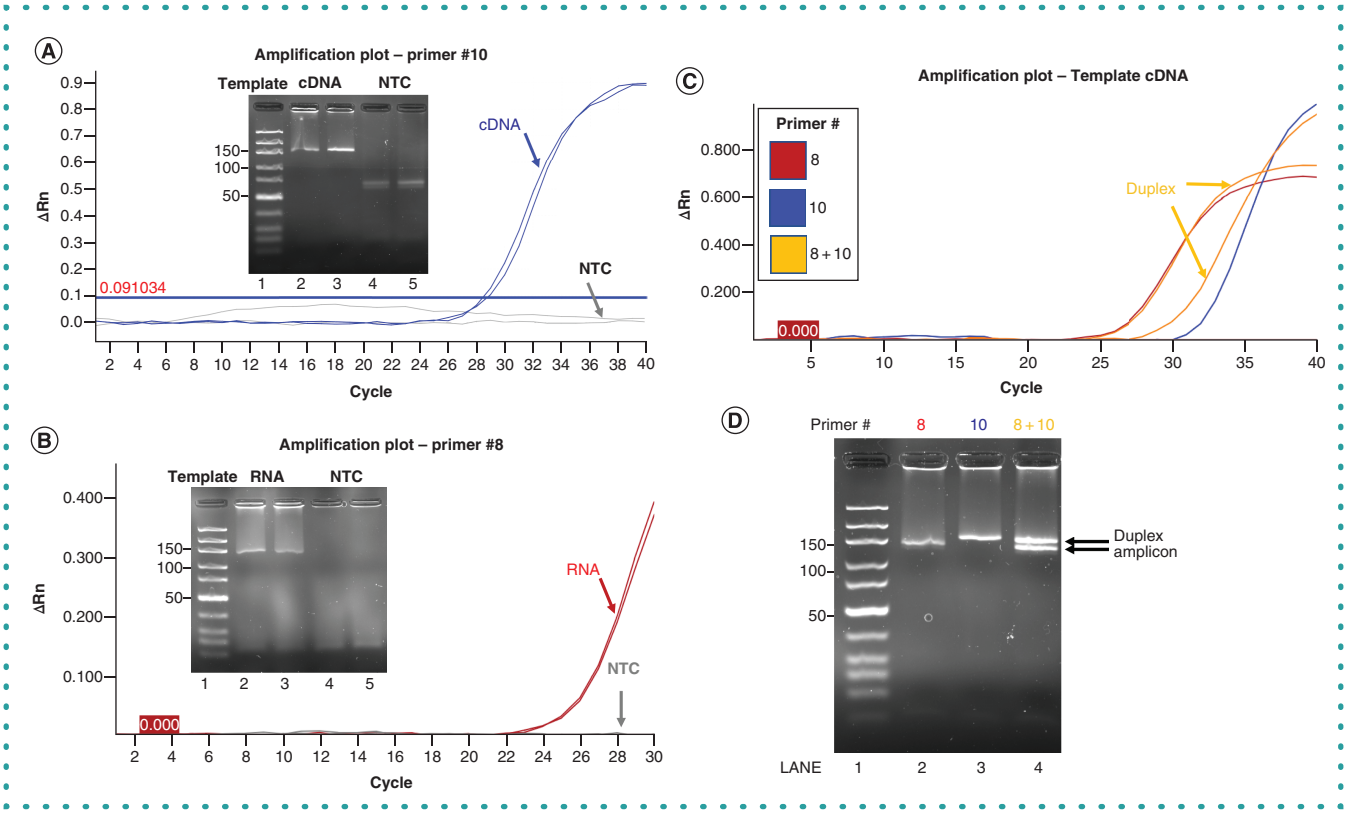

Figure 3. RT-PCR using double-bubble primers #8 and #10 with template SARS-CoV-2 synthetic RNA N and SARS-CoV-2 RNA under fast conditions. **(A)** qPCR using reverse-transcribed cDNA template and double-bubble (D-B) primer mix #10, FAM-TqM probe #13, TqM fast kit+ uracil-DNA glycosylase (UDG) assayed in duplicates. Insert depicts 5% agarose gel; lane 1: ultra-low-range (ULR) ladder; lanes 2 & 3: template cDNA; lanes 4 & 5: non-template control (NTC). C_t average values: cDNA, 28.60; NTC, undetermined. **(B)** One-tube RT-qPCR using SARS-CoV-2 synthetic RNA N template and D-B primer mix #8, VIC-TqM probe #12, TqM fast kit without UDG iScript reverse transcriptase, assayed in duplicate. Insert depicts 5% agarose gel; lane 1: ULR ladder; lanes 2 and 3: template RNA; lanes 4 and 5: NTC. C_t average values: RNA, 24.63, NTC, undetermined. **(C)** Duplex qPCR using SARS-CoV-2 synthetic RNA N template and TqM fast kit with UDG. C_t values: primer 8, 26.13; primer 10, 32.19; duplex primers 8 + 10, 26.36 and 30.27, respectively; NTC, undetermined. **(D)** 5% agarose gel of samples shown in panel C. Lane 1: ULR ladder; lane 2: primer D-B mix #8 (amplicon 139 bp); lane 3: D-B primer mix #10 (amplicon 158 bp); lane 4: duplex of both primers #8 and #10 (amplicons 139 and 158 bp). Arrows **(C & D)** show duplex amplifications in the same tube with D-B primers #8 and #10. PCR was performed using fast conditions with 40 **(A, C & D)** and 30 **(B)** cycles.

Cost–effectiveness of D-B PCR evaluation

With the advancement of the RT-PCR reaction, one of its most important components, Taq polymerase, has constantly improved, enhancing specificity, processivity and speed. As of today, most commercial PCR kits include the more advanced Taq polymerases. The improvements in Taq polymerase performance were naturally accompanied with increased prices: up to tenfold per unit between the most advanced compared with the original enzymes. Given that the D-B primers provide hot-start properties and hence improved specificity, we wished to explore this feature by comparing the D-B primers with conventional primers of matching size and configuration. In addition, we used the less expensive Taq polymerases without hot-start capabilities and introduced to the experiment less favorable PCR conditions (see Figure 6 legend) that are known to promote nonspecificity and reduced efficiency. Figure 6 shows an agarose gel of end point PCR reaction comparing four primers and two non-hot-start Taq polymerases (from NEB and FroggaBio) and cDNA template reverse-transcribed from synthetic RNA of the N gene of SARS-CoV-2. It can be seen that both Taq polymerase sources were generally comparable. D-B primer mix #8 exhibited the most robust and specific amplification with both enzyme sources, compared with the control primer mixes #5 (20-nt normal), #6 (30-nt normal) and #7 (20-nt sequence-specific plus 10-nt random). Primer mixes #5, #6 and #7 resulted in extra amplification bands and weaker signal. Note that *a priori*, a weaker signal was anticipated from primer mix #5 because it produces a shorter amplicon and hence lower reporter dye binding on the agarose gel. Taken together, this experiment demonstrates the advantage of the D-B primers compared with the control primers.

Next we wished to test the efficacy of the D-B primers in real-time qPCR with the non-hot-start Taq polymerases from NEB and Bio-Helix, and under fast conditions. Supplementary Figure 8 (upper panels) shows the amplification with D-B primer mix #8, using cDNA reverse transcribed from synthetic RNA of gene N of SARS-CoV-2 with NEB Taq polymerase. Supplementary Figure 8 (lower

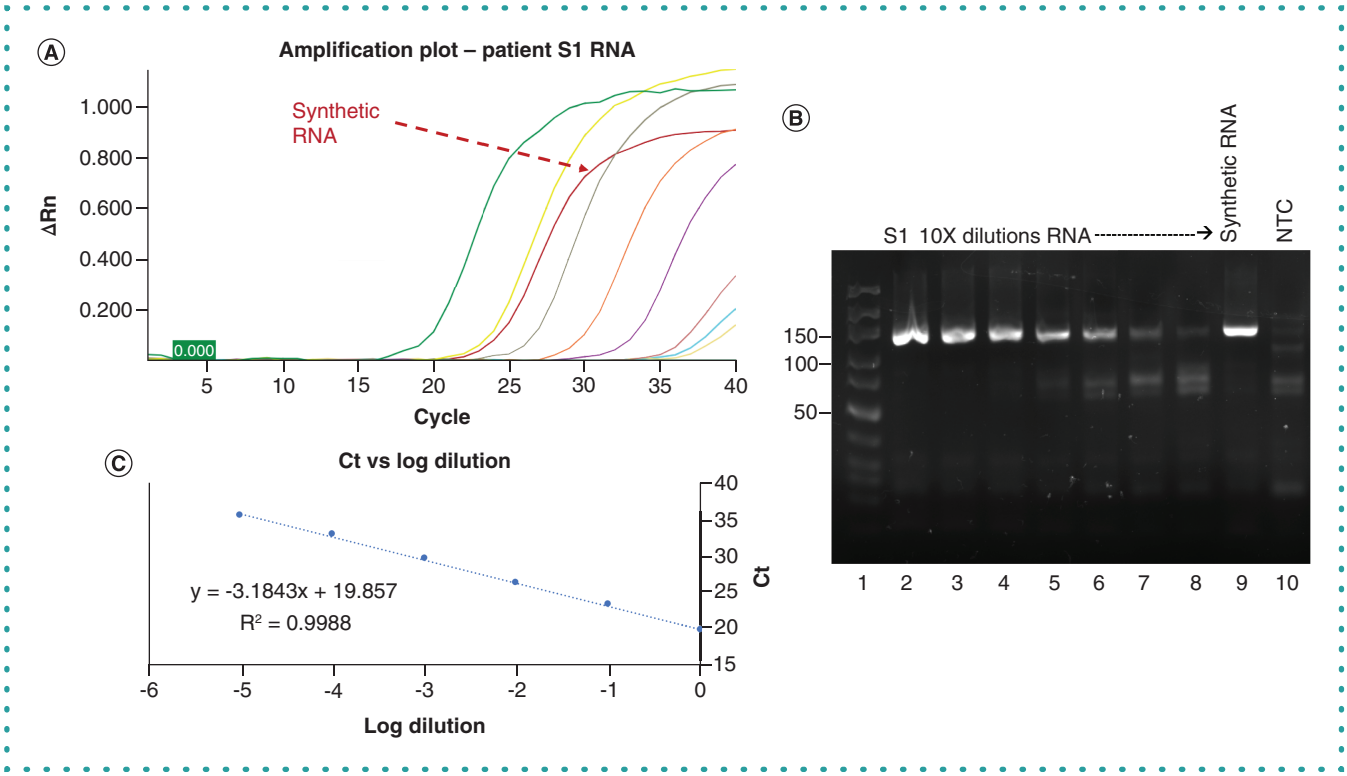

Figure 4. Dose–response curve for efficiency evaluation of double-bubble primer #8 using nasopharyngeal swab RNA under fast conditions. RNA extracted from nasopharyngeal swabs of patient S1 underwent decimal dilutions and was subjected to one-tube RT-qPCR utilizing fast TqM kit without uracil-DNA glycosylase, double-bubble primer mix #8 and VIC-TqM probe #12. Also used as controls were SARS-CoV-2 synthetic RNA N and non-template control (NTC). **(A)** Amplification plot. Arrow indicates amplification of synthetic RNA. **(B)** 5% agarose gel of the amplification products shown in panel A; lane 1: ultra-low-range ladder; lanes 2–8: decimal dilutions of virus RNA; lane 9: SARS-CoV-2 synthetic RNA N; lane 10: NTC. **(C)** Efficiency plot of C_t versus log RNA dilutions depicted in panel A (slope = -3.1843; R^2 = 0.9988; efficiency = 106.8%). Taking into consideration the dilution of the nasopharyngeal swab and using the synthetic RNA as guide, patient S1 has 1.4×10^6 virus RNA copies per microliter nasopharyngeal swab and the limit of detection is 3.76 SARS-CoV-2 virus copies per reaction. C_t values of decimal dilutions: 10: 19.71; 10^{-1}: 23.14; 10^{-2}: 26.12; 10^{-3}: 29.60; 10^{-4}: 32.83; 10^{-5}: 35.49; 10^{-6}: 36.39; synthetic RNA 2×10^4 copies: 24.31; NTC: undetermined. RT-qPCR was performed under fast conditions with 40 cycles.

panels) shows one-tube RT-qPCR using synthetic RNA of gene N of SARS-CoV-2 as a template. These results demonstrate that the D-B primers are compatible with the original Taq polymerase and with the TaqMan system under fast conditions.

In order to apply all the special improved features described above for the D-B primers, we performed one-tube real time RT-qPCR on RNA of nasopharyngeal swabs from patients who tested either positive or negative (Figure 7; lanes 2 and 3, respectively) for SARS-CoV-2 at St. Michael's Hospital molecular diagnostic lab. We also used non-template control (lanes 4 and 5) or synthetic RNA of gene N of SARS-CoV-2 (lane 6) as negative or positive controls, respectively. The reagents used in this experiment were D-B primer mix #4, Taq polymerase (FroggaBio), iScript reverse transcriptase, VIC-TqM probe #12, added dNTPs and ROX as reference dye. The reaction was assembled at room temperature and subjected to real time RT-qPCR using the following conditions: 42°C, 15 min → 95°C, 1 min; 30 cycles of 95°C, 1 s → 70°C, 20 s. After considering the volumes of the nasopharyngeal swabs and dilutions of the viral RNA taken for the assay, the volume of the RNA sample is equivalent to 0.067 μl of the nasopharyngeal swabs. Taken together, the results shown in Figure 7 demonstrate the fast, specific and robust attributes of the D-B primers and their compatibilities with cost-effective Taq polymerases for detecting SARS-CoV-2.

The difference between the melting temperature (95°C) and the annealing/extension temperature (70 vs 60°C, for the 20- and 30-nt primers) is lower for the D-B primers. This results in a 71.4% reduction in cycling time of D-B 30-nt primers compared with the 20-nt primers. Due to the robust qPCR amplification with the D-B primers, we were able to reliably use the reaction with 30 cycles. Compared with the 40 cycles used in regular qPCR reactions, this resulted in a further 75% reduction in cycling time using D-B primers compared with normal primers. Together, this could bring the total cycling time to about 50% using the D-B primers. Taken together, using cheaper Taq polymerases as shown here which are also compatible with fast PCR conditions with the D-B primers, renders the method cost-effective compared with the more expensive Taq polymerases that are used routinely in diagnostic kits.

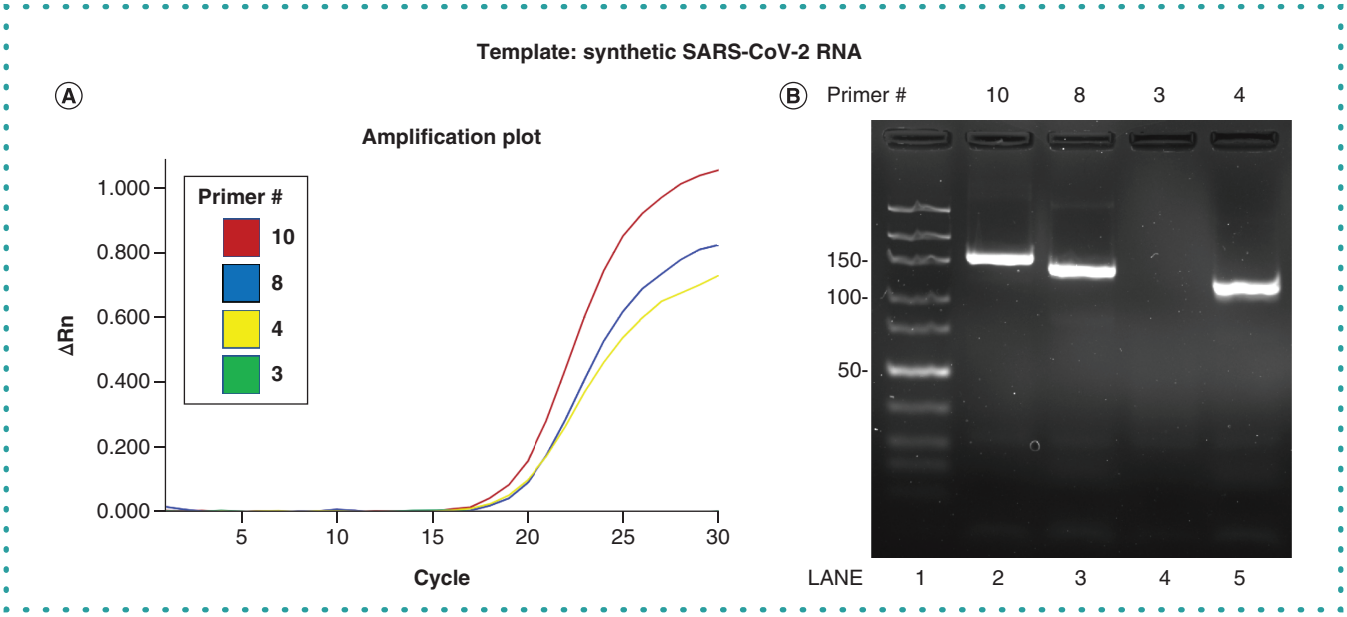

Figure 5. Comparison of double-bubble primers from different regions of SARS-CoV-2 gene N using the fast system. One-tube RT-qPCR was performed utilizing a fast TqM system without uracil-DNA glycosylase and RNA extracted from nasopharyngeal swabs of patient S3 as template, double-bubble (D-B) primer mix #10 with FAM-TqM probe #13 from region 2, D-B primer mixes #4 and #8 and normal primer mix #3 with VIC-TqM probe #12 from region 2. **(A)** Amplification plot. **(B)** 5% agarose gel of PCR products depicted in panel A. Lane 1: ultra-low-range ladder; lane 2: D-B primer #10 (amplicon 158 bp); lane 3: D-B primer #8 (amplicon 139 bp); lane 4: normal primer #3 (expected amplicon 96 bp); lane 5: D-B primer #4 (amplicon 115 bp). Note no amplification in lane 4 with normal primer mix #3, presumably because of the shorter standard primers that did not amplify under 70°C annealing/extension and the fast conditions. C_t values: primer #10, 19.24; primer #8, 19.75; primer #4, 19.44; primer #3 and non-template control, undetermined.

Using D-B primers to detect the N501Y mutation

The N501Y mutation has been detected in three variants of concern (VOC) – α, β and γ – that have been associated with increased transmissibility or detrimental change in COVID-19 epidemiology, possible increased virulence and decreased effectiveness of public health measures [14]. The method of choice for detecting VOCs is by on-site PCR and then genotyping the SARS-CoV-2 VOC by sequencing, usually utilizing off-site facilities. It could be useful to accelerate both the detection and genotyping calling by using the PCR machinery. We posited that the D-B primers might be useful for both detection and genotyping using RT-PCR. The amino acid asparagine is encoded by the codon aAT; the a→t mutation yields the codon tAT, which encodes tyrosine. Most advanced Taq polymerases employed in PCR reactions have proofreading 3′ to 5′ exonuclease activity which could remove the 3′ t nucleotide at the end of the mutant primer when it is used with a wild-type template and thus both mutant and wild-type viruses would yield a positive call. Hence using Taq polymerase without proofreading capabilities offers an advantage over the more advanced Taq polymerases. Our D-B primers' hot-start properties can replace Taq polymerases with hot-start capabilities. To demonstrate the proof of principle of the D-B primers for distinguishing between the wild-type and the mutated virus, we opted to use end point PCR. Although end point PCR is less sensitive than real-time qPCR, it is more accurate in detecting non-specific amplicons on agarose gels. In addition, in rural areas where access to expensive real-time PCR machines and reagents is limited, end point PCR is more affordable. To determine whether a D-B primer might be able to detect the N501Y mutation, we designed it with the point mutation a→t at the 3′ end, as described previously [15]. To confirm the D-B primer's utility with authentic patient samples, we ran a one-tube end point RT-PCR with RNA from N501Y-mutated VOC3 RNA extracted from nasopharyngeal swabs of patients with a confirmed mutation (Figure 8, lanes 2–4) or wild-type (Supplementary Figure 1, lanes 5–7). D-B primer mix #8 served as positive control (lanes 2 and 5). There is an obvious distinction between the bands' intensity when using wild-type or mutation primers with the opposite genotype RNA (compare lanes 3 vs 4 and lanes 6 vs 7 in Figure 8A; and the bands' densitometry in Figure 8B). These results suggest that wild-type and mutation primer mixes can be used for both detecting and genotyping an unknown nasopharyngeal swab using RT-PCR in the same run.

Here we have shown evidence for the existence of the D-B primers in stem–loop and homodimer configuration. This is important because this knowledge is crucial when considering parameters like annealing temperatures. The D-B primers are more specific than the conventional primers because they offer hot start at the pre-cycling phase of the PCR. In addition to our previously described hot-start primers [3], the D-B hot-start primers are designed with added improvement of the 3′ overhang that facilitates reverse transcription in addition to the PCR reaction. The D-B primers are 30 nt in size, longer than the traditional 20-nt primers, and as such produce a longer amplicon that enhances the signal both with real-time RT-qPCR and with end point agarose gels. While this feature also applies to the other

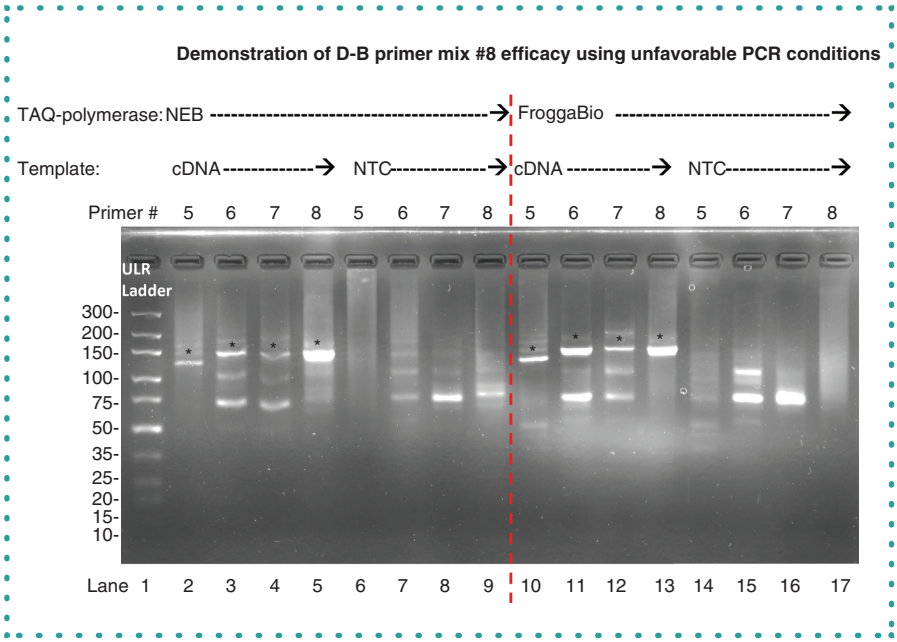

Figure 6. Efficacy and advantage of double-bubble primers compared with other comparable control primers using end point PCR. In order to demonstrate the advantage of the double-bubble (D-B) primers over other primers, we used comparable primers that control for primer size and configuration. Reactions were assembled under the following unfavorable PCR conditions: 1. Assembled and incubated 1 h at room temperature. 2. Taq polymerase from two sources (NEB and FroggaBio) without hot-start properties. 3. No hot-start procedure (e.g., inserting the PCR tube into the apparatus at high temperature). 4. High Taq polymerase concentration (1.25 U/10 μl reaction; five-times the recommended concentration). 5. High primer concentration (0.9 μM; 4.5- to nine-times the recommended concentration). 6. High Mg^{++} concentration (6 mM) (threefold than the recommended concentration). The primers that were compared with the D-B primer mix #8, all are from region 1 (Table S1 and Figure S2), each control different aspect of the D-B primers: Primer mix #5 are conventional 20 nt normal linear primers and are complimentary to the target template. Primer mix #6 contains 30-nt normal linear primers that are the same length as the D-B primers and all 30 nucleotides are complementary to the target template. Primer mix #7 contains 30-nt linear primers that are the same length as the D-B primer #8, the 20 nucleotides at the 3′ end are complementary to the target template and the 10 nucleotides at the 5′ end are random template-non-specific but do not assume D-B configurations. Primer mix #8 contains 30-nt D-B primers; the 20 nucleotides at the 3′ end are complementary to the target template and the 10 nucleotides at the 5′ end are random sequence non-specific but the 5′ end is designed to form a stem–loop and double-homo-primer configuration. Reverse-transcribed cDNA from synthetic SARS-CoV-2 RNA N was used as template with added 0.2 mM dNTPs. Lanes 2, 6, 10, 14: 20-nt sequence-specific primer mix #5 (amplicon 119 bp); lanes 3, 7, 11, 15: 30-nt sequence-specific primer mix #6 (amplicon 139 bp); lanes 4, 8, 12, 16: 30-nt primers mix #7 comprising 20-nt sequence-specific primers at the 3′ end plus 10-nt non-sequence-specific primers at the 5′ end (amplicon 139 bp); lanes 5, 9, 13, 17: D-B 30-nt primers comprising 20-nt sequence-specific primers at the 3′ end plus 10-nt non-sequence-specific primers at the 5′-end (amplicon 139 bp). Lanes 2–9: NEB Taq polymerase. Lanes 10–17: FroggaBio Taq polymerase. Asterisks designate expected migration of specific amplicon. Note the superior performance of the D-B primers compared with the other control primers in terms of specificity and robustness of the amplification. PCR conditions: 95°C,10 min; 40 cycles of 95°C,15 s→72°C,1 min; 72°C, 5 min; 4°C hold.

linear random-coiled 30-nt primers studied here (e.g., primer mixes #6 and #7; Supplementary Table 1), the D-B primers produce more robust and specific amplicons (Figure 6). Because of the longer primer size, the D-B primers can be used at higher annealing/extension temperatures (e.g., 70°C used here), which shortens the cycling phase and thus the overall reaction time. The hot-start characteristic of the D-B primers removes the need to use more expensive hot-start Taq polymerases, thereby lessening the expense of a PCR reaction. In addition, the less expensive non-hot-start Taq polymerases are efficient under fast PCR conditions which further makes them useful in accelerating the diagnostic results. Further, we showed that by using point-mutated primers, SARS-CoV-2 could be tested and genotyped simultaneously.

Future perspective

We would like readers, including private enterprises, to capitalize on the D-B primer concept and develop improved PCR-based kits for basic research of gene expression and rapid and affordable kits for medical diagnostic applications.

Conclusion

- Double-bubble primers exist in two configurations: stem–loop and primer dimers.
- Double-bubble primers contain three main features for efficient RT-PCR: 3′ overhang for reverse transcription, stem structure for PCR hot start and target-specific sequence for PCR amplification.

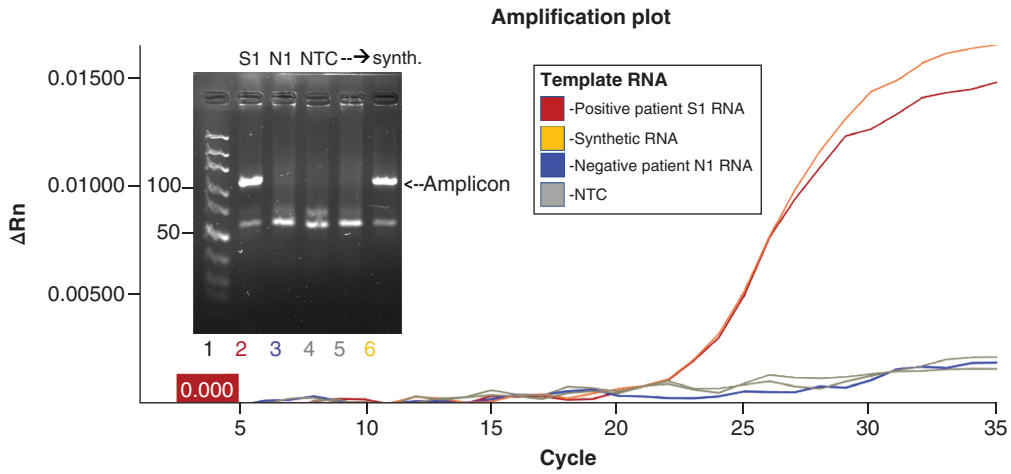

Figure 7. One-tube RT-qPCR demonstrating the fast, specific, cost-effective and robust attributes of the COVID-19 diagnostic assay with double-bubble primers. The reaction mixture contained hot-start double-bubble (D-B) primer mix #4, VIC-TqM probe #12, cost-effective non-hot-start Taq polymerase (FroggaBio), reverse transcriptase (iScript), synthetic SARS-CoV-2 RNA gene N as template, added dNTPs and ROX dye for internal calibration. The reaction was assembled at room temperature and subjected to real time RT-qPCR using the following fast conditions: 42°C, 15 min; 95°C,1 min; 30 cycles of 95°C, 1 s → 70°C, 20 s. The amplification plot and (insert) 5% agarose gel depict the amplification of SARS-CoV-2 RNA extracted from the nasopharyngeal swabs of patient S1 (lane 2) and negative patient N1 (lane 3), no-template controls (lanes 4 and 5) and SARS-CoV-2 gene N synthetic RNA as positive control (lane 6). Note the amplification in the real-time plot and the 115-bp band in the 5% agarose gel with SARS-CoV-2 virus or synthetic RNA (lanes 2 and 6), with no amplifications in the negative control N1 (lane 3) or NTC (lanes 4 and 5). Lane 1: ultra-low-range ladder. C_t values: positive patient S1: 23.95; synthetic RNA: 23.84; negative patient N1 and NTC: undetermined.

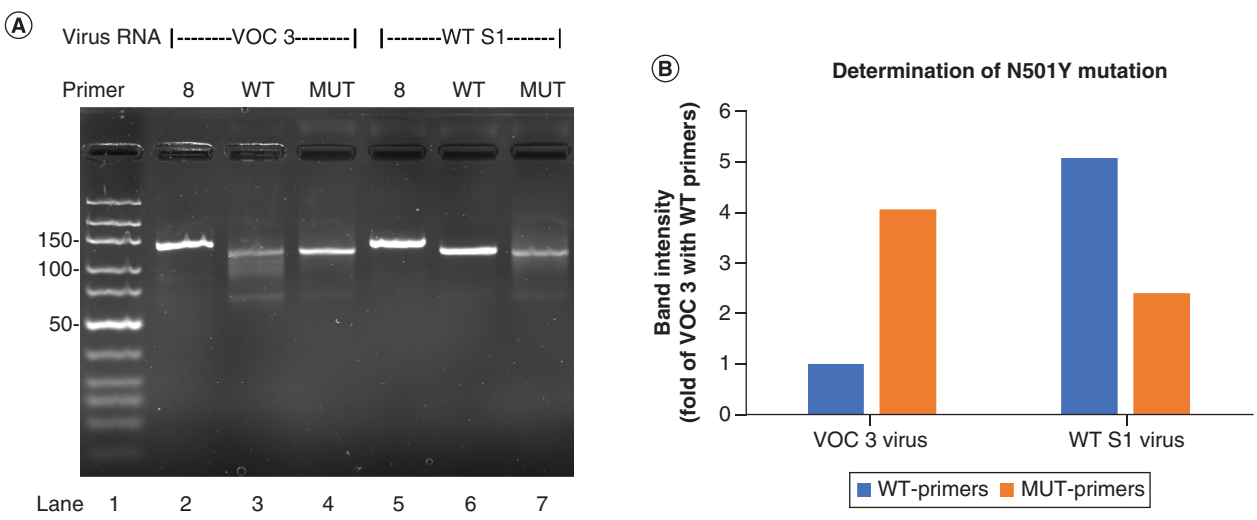

Figure 8. Utilizing double-bubble primers in RT-qPCR to detect N501Y mutation using end point RT-PCR. (A) 5% agarose gel showing detection of SARS-CoV-2 N501Y-mutated RNA extracted from nasopharyngeal swabs of patient VOC3 or wild-type viral RNA extracted from nasopharyngeal swabs from patient S1. Templates for PCR reactions: lanes 1 and 8: ultra-low-range ladder; lanes 2–4: VOC3 RNA; lanes 5–7: S1 RNA, lanes 9 and 10: non-template control. Primer mixes: lanes 2 and 5: region 1 gene N primer mix #8 positive controls; lanes 3, 6, 9: region 3 gene S wild-type primer mix #11a + #11c; lanes 4, 7, 10: region 3 gene S N501Y mutation (MUT) primer mix #11b + #11c. **(B)** Densitometry of the agarose bands depicted in lane A. We designed a double-bubble primer with the point mutation a→t at the 3′ end to detect the viral point mutation. In addition, we introduced a c→t mismatch mutation at position -5 of the 3′ overhang to lower the annealing intensity of the sense primers to the opposite genotype. Wild-type sense primer #11a has base 'a' at the 3′ end (Supplementary Table 1). Sense primer #11b has a point mutation 't' at the 3′ end to detect the a→t replacement of the N501Y mutation. These results suggest that these two primer mixes can be used for both detecting and genotyping an unknown nasopharyngeal swab using RT-PCR in the same run. Furthermore, by adding to the genotyping primers a primer mix from a non-mutated region of the virus (e.g., primer mix #8), it will be possible to determine by duplex PCR the genotype and the level of the virus simultaneously. The RNA from the nasopharyngeal swabs of the wild type S1 and the VOC3 viruses were initially sequenced by the St. Michael's Hospital diagnostic lab, and confirmed by us by sequencing the purified RT-PCR amplicons at the Centre for Applied Genomics DNA Sequencing Facility (Hospital for Sick Children, Toronto, Canada).

- Double-bubble primers offer fast, specific and robust improvement in PCR amplification and are compatible with cost-effective Taq polymerases.
- We show evidence that double-bubble primers are useful in detection of gene expression in general, and detection and genotyping of SARS-CoV-2 in particular.

Supplementary data

To view the supplementary data that accompany this paper please visit the journal website at: www.future-science.com/doi/suppl/10.2144/btn-2021-0063

Author contributions

M Ailenberg conceived and designed the study, performed the experiments, analyzed and interpreted the data and drafted the manuscript and figures. A Kapus critically evaluated the manuscript, analyzed and interpreted the data, drafted the manuscript and funded the study. O Rotstein provided general guidance, analyzed and interpreted the data, drafted the manuscript, co-ordinated and funded the study.

Acknowledgments

The authors would like to acknowledge the Keenan Research Centre Core Facilities at St. Michael's Hospital, especially P Plant and C Di Ciano-Oliveira, for their expert technical support and encouragement. They would also like to thank the staff of St. Michael's molecular diagnostic laboratory for their collaboration and supplying the SARS-CoV-2 nasopharyngeal swabs.

Financial & competing interests disclosure

This study was supported by a grant from the St. Michael's Hospital Foundation (O Rotstein, A Kapus) and a grant from CIHR # 400642 (O Rotstein). The authors have no other relevant affiliations or financial involvement with any organization or entity with a financial interest in or financial conflict with the subject matter or materials discussed in the manuscript apart from those disclosed.

No writing assistance was utilized in the production of this manuscript.

Ethical conduct of research

This study was conducted in accordance with the guidelines of Unity Health Toronto Research Ethics Board (REB) for studies involving human subjects. All samples were de-identified and therefore no informed consent from subjects was required.

References

Papers of special note have been highlighted as: •• of considerable interest

1. Vallone PM, Butler JM. AutoDimer: a screening tool for primer-dimer and hairpin structures. *BioTechniques* 37(2), 226–231 (2004).
2. Paul N, Shum J, Le T. Hot start PCR. *RT-PCR Protocols*. In: *Methods in Molecular Biology.* Humana Press 630, 301–318 (2010).
3. Ailenberg M, Silverman M. Controlled hot start and improved specificity in carrying out PCR utilizing touch-up and loop incorporated primers (TULIPS). *BioTechniques* 29(5), 1018–1024 (2000).

•• **First paper showing the advantage of stem–loop primers in hot-start and touch-up PCR.**

4. Varkonyi-Gasic E, Wu R, Wood M *et al.* Protocol: a highly sensitive RT-PCR method for detection and quantification of microRNAs. *Plant Methods* 3, 12 (2007).
5. Wong ML, Medrano JF. Real-time PCR for mRNA quantitation. *BioTechniques* 39(1), 75–85 (2005).
6. Hu B, Guo H, Zhou P, Shi Z-L. Characteristics of SARS-CoV-2 and COVID-19. *Nat. Rev. Microbiol.* 19(3), 141–154 (2021).
7. Wang R, Hozumi Y, Yin C, Wei GW. Mutations on COVID-19 diagnostic targets. *Genomics* 112(6), 5204–5213 (2020).
8. Orbons LPM, van der Marel GA, van Boom JH, Altona C. Hairpin and duplex formation of the DNA octamer d(m C-G-m C-G-T-G-m C-G) in solution. An NMR study. *Nucleic Acids Res.* 14(10), 4187–4196 (1986).
9. Kaboev OK, Luchkina LA, Tret'iakov AN, Bahrmand AR. PCR hot start using primers with the structure of molecular beacons (hairpin-like structure). *Nucleic Acids Res.* 28(21), e94 (2000).

•• **First paper showing the advantage of stem–loop primers in hot-start PCR.**

10. Farahani N, Behmanesh M, Ranjbar B. Evaluation of rationally designed label-free stem–loop DNA probe opening in the presence of miR-21 by circular dichroism and fluorescence techniques. *Sci. Rep.* 10(1), 4018 (2020).
11. Nakano S-iN, Hirayama H, Miyoshi D, Sugimoto N. Dimerization of nucleic acid hairpins in the conditions caused by neutral cosolutes. *J. Phys. Chem. B* 116(25), 7406–7415 (2012).
12. Zhao H, Magone MT, Schuck P. The role of macromolecular crowding in the evolution of lens crystallins with high molecular refractive index. *Phys. Biol.* 8(4), 046004 (2011).
13. Sun Y, Li Y, Luo D, Liao DJ. Pseudogenes as weaknesses of ACTB (Actb) and GAPDH (Gapdh) used as reference genes in reverse transcription and polymerase chain reactions. *PLoS ONE* 7(8), e41659 (2012).
14. World Health Organization. Tracking SARS-CoV-2 variants. **http://www.who.int/en/activities/tracking-SARS-CoV-2-variants**
15. Newton CR, Graham A, Heptinstall LE *et al.* Analysis of any point mutation in DNA. The amplification refractory mutation system (ARMS). *Nucleic Acids Res.* 17(7), 2503–2516 (1989).